

# Embedded Wireless Sensor Design for Long Term Structural Health Monitoring

Christopher Bessin<sup>2</sup>, Patrick Blum<sup>1</sup>, Matthew P. Iannucci<sup>1</sup>, Jordan T. Kirby<sup>1</sup>, Zachary McIntosh<sup>1</sup>, Elizabeth L. Paul<sup>2</sup>, Michael A. Regan<sup>1</sup>, Justin W. Skenyon<sup>2</sup>, Charles J. Wesley<sup>1</sup>, and Samuel D. Wiley<sup>1</sup>

<sup>1</sup>Finite Element Modelling

<sup>2</sup>Instrumentation Development

May 4, 2014

*I have read this paper in its entirety and approve it for submission.*

---

Christopher Bessin

Date

---

Patrick Blum

Date

---

Matthew P. Iannucci

Date

---

Jordan T. Kirby

Date

---

Zachary McIntosh

Date

---

Elizabeth L. Paul

Date

---

Michael A. Regan

Date

---

Justin W. Skenyon

Date

---

Charles J. Wesley

Date

---

Samuel D. Wiley

Date

# Contents

<b>1</b>	<b>Introduction</b>	<b>6</b>
1.1	Objectives . . . . .	6
1.1.1	Phase One . . . . .	6
1.1.2	Phase Two . . . . .	6
1.2	Layout . . . . .	6
<b>2</b>	<b>Finite Element Model (FEM)</b>	<b>7</b>
2.1	Introduction . . . . .	7
2.1.1	Background of Claiborne Pell Bridge . . . . .	7
2.1.2	Introduction of FEM . . . . .	7
2.2	Abaqus FEM Verification . . . . .	7
2.2.1	L Beam Analysis . . . . .	7
2.3	Claiborne Pell Bridge Model . . . . .	7
2.3.1	Modeling Large Suspension Bridges . . . . .	7
2.3.2	Model Process . . . . .	7
2.3.3	Limitations of Abaqus FEM . . . . .	7
<b>3</b>	<b>Instrumentation Package</b>	<b>8</b>
3.1	Introduction . . . . .	8
3.2	Microprocessor . . . . .	8
3.2.1	Necessary Specifications . . . . .	8
3.2.2	Platform Options . . . . .	8
3.2.3	Final Platform . . . . .	8
3.3	Sensors . . . . .	8
3.3.1	Accelerometer . . . . .	8
3.3.2	Strain Gauge . . . . .	8
3.3.3	GPS Receiver . . . . .	8
3.3.4	CORS . . . . .	9
3.3.5	Analog to Digital Converter . . . . .	9
3.4	Electronics Design . . . . .	9
3.4.1	Introduction . . . . .	9
3.4.2	Circuitry . . . . .	9
3.4.3	Printed Circuit Board . . . . .	10
3.5	Software Design . . . . .	10
3.6	Package Power . . . . .	10

3.6.1	Power Budget . . . . .	10
3.6.2	Energy Scavenging Potential . . . . .	10
3.6.3	Battery Selection . . . . .	10
<b>4</b>	<b>Data Collection</b>	<b>11</b>
4.1	Phase One Data Collection . . . . .	11
4.1.1	6g Tri-Axial Accelerometer Data . . . . .	11
4.2	Phase Two Data Collection . . . . .	11
4.2.1	6g Tri-Axial Accelerometer Data . . . . .	11
4.2.2	1.5g Tri-Axial Accelerometer Data . . . . .	11
4.2.3	Cell Phone Accelerometer . . . . .	11
4.2.4	Battery Discharge Curve . . . . .	11
4.2.5	Experimental Observed Efficiency . . . . .	11
<b>5</b>	<b>Data Analysis</b>	<b>12</b>
5.1	Phase One Data Analysis . . . . .	12
5.1.1	Comparison of Preliminary Abaqus Model and Preliminary Data . . .	12
5.2	Phase Two Data Analysis . . . . .	12
5.2.1	Comparison of Developed Abaqus Model with Literature . . . . .	12
5.2.2	Comparison of Developed Abaqus Model with Developed Abaqus Model	12
<b>6</b>	<b>Future Development</b>	<b>13</b>
6.1	Instrumentation . . . . .	13
6.1.1	Integration of Strain Gauge . . . . .	13
6.1.2	Wireless Transmission . . . . .	14
6.1.3	GPS Time Synchronization . . . . .	14
6.1.4	Package Assembly . . . . .	14
6.2	Package Enclosure . . . . .	14
6.3	Package Location . . . . .	19
6.4	FEM . . . . .	21
6.4.1	Model Improvements . . . . .	21
6.4.2	Dynamic Loading . . . . .	21
<b>7</b>	<b>Conclusion</b>	<b>23</b>
<b>A</b>	<b>Sensor Package Schematics</b>	<b>25</b>
A.1	BeagleBone Black . . . . .	26
A.2	Trimble Copernicus II GPS Receiver . . . . .	27
A.3	ADS1113 Analog-Digital Converter . . . . .	29
A.4	LM317 Adjustable Voltage Regulators . . . . .	30
A.5	MMA7361 Accelerometer . . . . .	31
<b>B</b>	<b>Enclosure Options</b>	<b>32</b>

# List of Figures

6.1	Omega 3-Element Rosette with pre-soldered leads. . . . .	14
6.2	Example Mating Mechanisms . . . . .	16
6.3	USB 2.0A External Connector (LTWUA-20AMFM-SL7A) from Ampehnol LTW . . . . .	17
6.4	Shielded Ethernet External Connector (RJ45-5EWTP-QR-PCB) from Video Production Inc . . . . .	17
6.5	Cable Gland (CB-GD-5000045) from AA Power Corp . . . . .	17
6.6	MCX Jack-to-Jack Adapter (252171) from Aamphenol Connex with Size Reference . . . . .	18
6.7	Waterproof SMA Bulkhead Connector (9153-7553-002) from Applied Engineering Products with Size Reference . . . . .	18
6.8	Potential Layout of a Pelican 1400 Model Case . . . . .	20
6.9	Neodymium Mounting Magnet. . . . .	21
6.10	Proposed Package Mounting Location. . . . .	21
6.11	Proposed Location for Sensor Package, Wind Turbine and Solar Panels. . . . .	22
A.1	Schematic of BeagleBone Black . . . . .	26
A.2	Schematic of Copernicus II GPS Receiver . . . . .	27
A.3	Schematic of four ADS1113 ADC units in parallel . . . . .	29
A.4	Schematic of 5V and 3.3V voltage regulator circuit . . . . .	30
A.5	Schematic of MMA7361 $\pm 1.5g$ / $\pm 6g$ Tri-Axial Accelerometer . . . . .	31

# List of Tables

3.1	LM317 Adjustable Linear Regulator Specifications . . . . .	9
B.1	Brief summary of enclosure options considered for the sensor package . . . . .	33

# Chapter 1

## Introduction

### 1.1 Objectives

#### 1.1.1 Phase One

#### 1.1.2 Phase Two

### 1.2 Layout

# Chapter 2

## Finite Element Model (FEM)

### 2.1 Introduction

2.1.1 Background of Claiborne Pell Bridge

2.1.2 Introduction of FEM

### 2.2 Abaqus FEM Verification

2.2.1 L Beam Analysis

### 2.3 Claiborne Pell Bridge Model

2.3.1 Modeling Large Suspension Bridges

2.3.2 Model Process

2.3.3 Limitations of Abaqus FEM

# Chapter 3

## Instrumentation Package

### 3.1 Introduction

### 3.2 Microprocessor

#### 3.2.1 Necessary Specifications

#### 3.2.2 Platform Options

#### 3.2.3 Final Platform

### 3.3 Sensors

#### 3.3.1 Accelerometer

Necessary Specifications

Sensor Options

Sensor Selection

#### 3.3.2 Strain Gauge

Necessary Specifications

Sensor Options

Sensor Selection

#### 3.3.3 GPS Receiver

Necessary Specifications

Sensor Options

Sensor Selection

### 3.3.4 CORS

#### 3.3.5 Analog to Digital Converter

Necessary Specifications

Platform Options

## 3.4 Electronics Design

### 3.4.1 Introduction

The unique requirements for the sensor developed for deployment on the Claiborn Pell Newport Bridge set the sensor apart from off-the-shelf sensors readily available for purchase. The sensor package needed to record high precision, high resolution accelerometer and strain gauge data continuously for an extended period of time. The longevity of the package was dependent upon the battery capacity and data storage capacity. This could have been solved by utilizing a large bank of batteries and multiple hard disk drives; however it was determined that this was not a feasible option. Instead the sensor package would scavenge energy to recharge batteries and transmit data to a base station wirelessly. The addition of these two requirements greatly increased the complexity of the sensor package design.

### 3.4.2 Circuitry

#### Voltage Regulation

The voltage input for most systems on the sensor board are a range of voltages between 3.3V-5V. This posed a basic issue due to the output voltage of the 12V battery. The solution was to use two LM317 linear voltage regulators. The LM317 technical specifications are displayed in Table 3.1

Parameter	Value
Input Voltage Differential ( $V_{in} - V_{out}$ )	$3V \leq V_{in} - V_{out} \leq 40V$
Output Voltage ( $V_{out}$ )	$1.2V \leq V_{out} \leq 37V$
Output Current ( $I_{out}$ )	1.5A
Max Power Dissipation ( $P_D$ )	20W
Package Type	TO-220

Table 3.1: LM317 Adjustable Linear Regulator Specifications

The output voltage can be set using Equation 3.1 where  $R_1$  and  $I_{adj}$  are typically  $240\Omega$  and  $\leq 100\mu A$  respectfully. It should be noted the  $V$  is not the input voltage, but a unit placeholder and

$$V_{out} = 1.25V(1 + \frac{R_2}{R_1}) + I_{adj}R_2 \quad (3.1)$$

### **3.4.3 Printed Circuit Board**

## **3.5 Software Design**

## **3.6 Package Power**

### **3.6.1 Power Budget**

### **3.6.2 Energy Scavenging Potential**

Wind Potential

Solar Potential

### **3.6.3 Battery Selection**

# **Chapter 4**

## **Data Collection**

### **4.1 Phase One Data Collection**

#### **4.1.1 6g Tri-Axial Accelerometer Data**

### **4.2 Phase Two Data Collection**

#### **4.2.1 6g Tri-Axial Accelerometer Data**

#### **4.2.2 1.5g Tri-Axial Accelerometer Data**

#### **4.2.3 Cell Phone Accelerometer**

#### **4.2.4 Battery Discharge Curve**

#### **4.2.5 Experimental Observed Efficiency**

# **Chapter 5**

## **Data Analysis**

### **5.1 Phase One Data Analysis**

#### **5.1.1 Comparison of Preliminary Abaqus Model and Preliminary Data**

### **5.2 Phase Two Data Analysis**

#### **5.2.1 Comparison of Developed Abaqus Model with Literature**

#### **5.2.2 Comparison of Developed Abaqus Model with Developed Abaqus Model**

# Chapter 6

## Future Development

### 6.1 Instrumentation

#### 6.1.1 Integration of Strain Gauge

##### Integration of Strain Gauge

Figure 6.1 is one of the 3-element rosette strain gauges with pre-soldered ribbon leads. Purchased from omega engineering with model number SGD-6/120RYT23. These strain gauges were necessary after realizing the difficulty of soldering leads to the original set of strain gauges. The pre-soldered ribbon leads on the second set of strain gauges also proved to be unsuccessful during experimentation. This was because the leads would not stay secured to the attaching clips while tests were being run. Even with the persistent attempts to get the strain gauges connected and working correctly, the data received was still very inaccurate. One possible contributing factor to this may have been the lack of precision when applying the strain gauge to the exact location on the beam. However, one definite factor that contributed to the inaccurate data from the strain gauges was the type of strain gauge that was used. A strain gauge with a different gauge factor and a higher resistance would have been more favorable. The higher the resistance of a strain gauge, the higher the sensitivity. The original sets of strain gauges had a resistance of  $120\ \Omega$ , but to precisely measure strain on a beam the resistance must be much higher,  $350\ \Omega$  or more. The costs for a pack of 6 similar strain gauges with a resistance of  $350\ \Omega$  from omega engineering is one hundred dollars. Another factor that halted the efforts to apply the strain gauge was that they required another ADC output. It is possible to make more outputs, however this also demands that the time synchronization is even more accurate. Nevertheless, higher resistant strain gauges would be better for sensor packages for future developments.

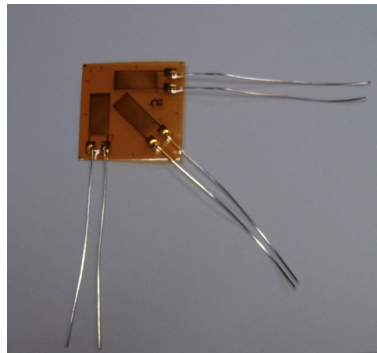


Figure 6.1: Omega 3-Element Rosette with pre-soldered leads.

### 6.1.2 Wireless Transmission

### 6.1.3 GPS Time Synchronization

### 6.1.4 Package Assembly

Fabrication of Circuit Board

Battery Integration

Power Management

Package Enclosure

## 6.2 Package Enclosure

When the components are tested and fully operational in laboratory conditions, they will need to be packaged into the casing. The following characteristics need to be considered when determining which case is best suited for this application:

- Quality
- Size/Orientation
- Heat Dissipation
- Cost
- External Connectors

When the package is mounted onto the Newport Bridge, it will be exposed to harsh weather conditions: wind, precipitation, extreme temperatures, etc. Therefore, it is essential to utilize a case that can withstand these conditions. O-rings are necessary to prevent water from leaking into the case through the seal of the lid. This water can easily damage the electrical components within the package. The case will also have to be able to withstand possible extreme temperatures. If the case cannot withstand the possible cold temperatures it will be exposed to without cracking, water can leak into the package and destroy the

equipment. High temperatures can cause the case to melt/deform which may possibly affect the retrieved data.

It will be important to choose a case that not only large enough that can house all of the equipment but also fits the equipment in a manner that it can be neatly organized and arranged. This allows for a quicker and more efficient package assembly. This also allows for a quicker examination of the set-up in case an error occurs. To account for this, the orientation of the case is important. For example, a top-loading bucket (such as the Pelican 1430 seen below) would not be practical because it would be very difficult to access the components once the package is assembled and mounted.

Electrical devices are only operational within a specific temperature range where if the maximum or minimum temperatures are exceeded, the component may not fully function or even fail completely. To determine if the SHM system will fail due to extreme temperatures, the temperature inside the case must be calculated. The enclosed volume has two major sources of temperature flux: the external temperature and the work done by the system. The first step will be to calculate the heat transferred from the electrical components using the equation:

$$q(eq) = P(eq) * K_1 * K_2 \quad (6.1)$$

where  $q(eq)$  is the heat transferred from electrical equipment in Watts (W),  $P(eq)$  is the electrical power consumption (W),  $K_1$  is the load coefficient, and  $K_2$  is the running time coefficient. This value will then be inserted into the 1-D heat transfer equation:

$$q = k * A * \frac{\Delta T}{dx} \quad (6.2)$$

where  $q$  is the heat due to the electrical components,  $k$  is the thermal conductivity of the material,  $A$  is the area of which heat is being transferred through,  $\Delta T$  is the change in temperature, and  $dx$  is the thickness of material. This equation will need to be computed for the heat transfer through each of the casing walls, as well as the corners of the case, then averaged using the equation:

$$q_t = \sqrt{(q_x)^2 + (q_y)^2 + (q_z)^2 + (q_c)^2}$$

where  $q_c$  is the heat transfer through the corners of the case. The resulting value will then be used with the maximum expected temperatures based on temperature history data, such as that provided by NOAA, to determine the maximum temperature at which the system will still operate. If the resulting temperature is higher than the lowest maximum operating temperature out of all the components, the system may fail, and that case may not be the best option. That same principal can be applied to when the system is not generating any heat with respect to the minimum expected external temperature and highest minimum operational temperature of the components. Ideally, once the package is fully modeled, the heat transfer equation can be more thoroughly and accurately calculated by accounting for the spatial orientation between the components and the interior walls of the case. However, if the components are mounted in place via foam cutouts, the heat dissipation between the components and the foam must first be calculated, and then the heat transfer between the foam and the interior walls will then be calculated.

**External Connectors** Several external connectors will need to be installed on the case walls for the full functionality of the SHM system. These ports need to be waterproof with tight seals to prevent water from entering the case or external connections. The waterproof connections will require secure mating mechanisms, such as locking and screwing mechanisms shown in Figure 6.2, to ensure that the male ends will not become unplugged thus allowing water to enter the connection and damage it. Each connector will also require a bulkhead cap to cover and protect against water damage if the connector is not in use. These external connections are going to be implemented for a variety of sub-systems within the SHM package: energy scavenging devices, BeagleBone Black, strain gauge, GPS, and XBee.



Figure 6.2: Example Mating Mechanisms

Power connectors will be used to connect the wind turbine and solar panels to the package. These connectors must be rated for a high enough current to match the power source. For example, since the wind turbine is rated up to 27A, the power connector should have a current rating that is similar enough that there will not be damage done to the port due to the excess current. Each power connection will have a female port installed on the side of the case and a corresponding male jack will need to be installed at the end of the power input. If multiple solar panels are utilized, either the power inputs need to be put into parallel in one wire to input all the energy through one connection or a connector needs to be installed for as many panels are used.

A USB 2.0A port will be installed to access the BBB without having to open the package via a flash drive. This type of USB port was chosen to match the same type of connection specified from the BBB data sheet. The connector gender of this port needs to be female to plug a USB chord to access the BBB, such as the one seen in Figure 6.3.

There are a few different types of connectors that can be used to attach the leads of the strain gauge to the package. Unlike the rest of the connections, the strain gauge leads do not require a certain type of connection terminal. One option is to attach the leads to either a category 5 (CAT 5) or CAT5e shielded Ethernet cable and install an external connection for such a cable as seen in Figure 6.4. Category type cables are designed for high signal integrity to achieve performance standards set by organizations [1]. This type of cable will ensure that the signals are relayed to the ADC reliably. A shielded cable is desired to ensure that the sensitive signal being sent from the strain gauge to the ADC does not get disturbed by noise.



Figure 6.3: USB 2.0A External Connector (LTWUA-20AMFM-SL7A) from Ampehnol LTW



Figure 6.4: Shielded Ethernet External Connector (RJ45-5EWTP-QR-PCB) from Video Production Inc

An alternative method is through the use of waterproof cable glands (see Figure 6.5). The leads would be attached to a cable, preferably shielded, and fed through the gland which would then be sealed. The proper gland must be matched up to the outer diameter of the cable otherwise the gland will not be water tight. These are advantageous because not only do individual cable glands work with a range of cable thicknesses, but different gland diameter ranges can be found.

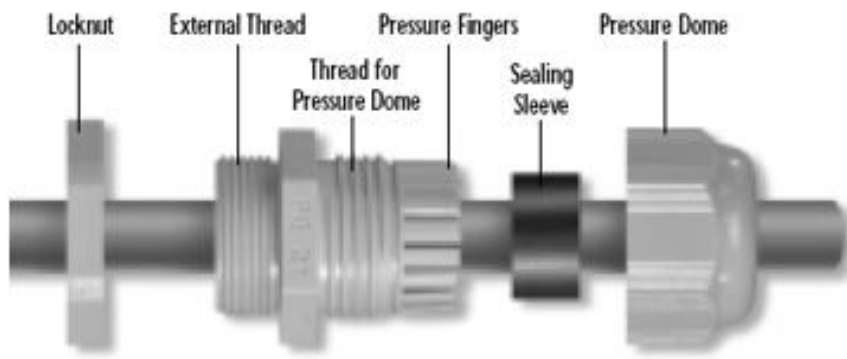


Figure 6.5: Cable Gland (CB-GD-5000045) from AA Power Corp

The GPS antenna attaches to the GPS via the use of a coaxial MCX connection. Two viable options for connecting the antenna are to implement a waterproof MCX connector or a cable gland. Implementing a waterproof MCX connector on the package may be difficult

because MCX connectors are very small as evident by Figure 6.6. If one of these connectors is able to implemented, it will be essential to choose the proper impedance level of the connector. The other option is to implement a cable gland, such as the alternative option for the strain gauge above in Figure 6.5, to run a wire through the case wall between the antenna and the GPS. The antenna would then need to be fastened to the outside of the case or another substrate to prevent it from freely swinging around.

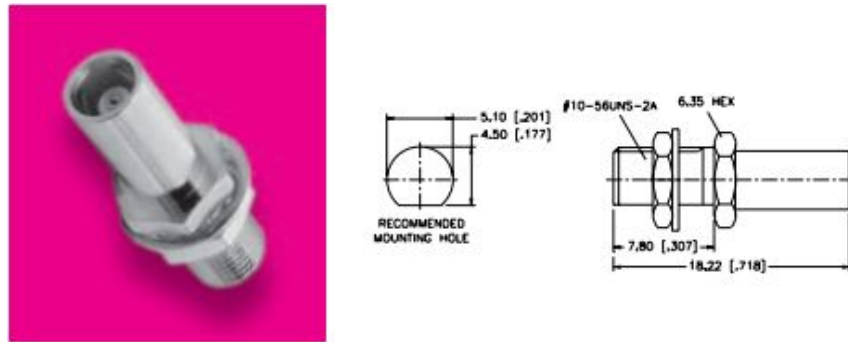


Figure 6.6: MCX Jack-to-Jack Adapter (252171) from Aamphenol Connex with Size Reference

The final component that requires an external connector is the XBee. The XBee antenna attaches to the device itself via the use of an SMA connection. A waterproof coaxial connector, like the one shown in Figure 6.7, can be implemented as the external connector as well as a cable gland. Similarly to the MCX connector, the SMA connector is also small which may make utilizing one of these difficult. However, if a cable gland is used, the antenna may need to be mounted to the case or other substrate to prevent it from freely swinging around as is the case with the GPS.

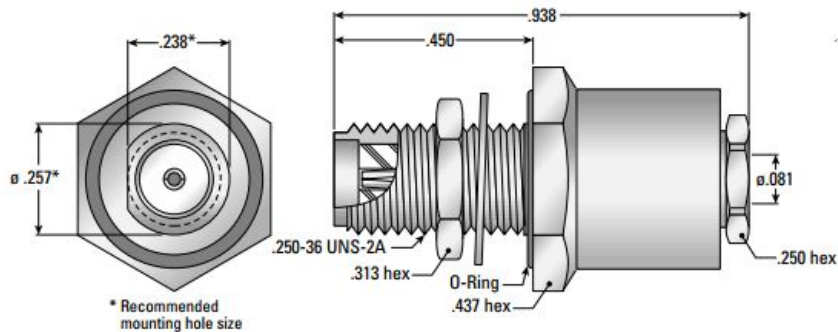


Figure 6.7: Waterproof SMA Bulkhead Connector (9153-7553-002) from Applied Engineering Products with Size Reference

**Case Selection** Attempts were made to try to obtain the actual thermal conductivity coefficients for different cases, but unfortunately proper data was never able to be retrieved due to lack of information from retailers. Since the general material of the considered cases is known, an estimation of the thermal conductivity coefficient was made because studies have

been performed to determine  $k$  values for different materials. However, continued efforts to obtain this information may supply data to more accurately calculate the heat transfer through the casing walls. The thickness of each case will need to be considered for two reasons. The first reason is that the thickness of the case affects heat transfer. Thicker cases will allow for less heat transfer through the casing walls. The other is that the thickness of the casing wall affects whether or not certain external connectors can be implemented. If the case is too thick, many MCX and SMA connectors may not be able to be installed because the case may be thicker than the connector is long. When comparing costs, it should be later noted of any accessories, whether they are necessary or convenient, that can and will be purchased. For example, the Ultra-case 613 by UW Kinetics charges another \$6.99 for the required O-ring to water proof an already expensive case, so this may not be the most suitable case for this application. For a look at the a comparison of nominal characteristics of the cases that were considered, see ??.

**Assembly Layout** When the package is ready to be assembled, the interior layout of the components needs to be determined. A few factors will need to be considered. The first is the location of external connectors. As stated above, the thickness of the case will affect what type of connectors may need to be used. An example of this is shown in Figure 6.8 which is a potential 2-D assembly layout using a Pelican 1400 model case. If an SMA connector is used instead of a cable gland, it would need to be installed on the shorter wall since the case does not have a uniform thickness and that wall is the only one thin enough out of the two to install such a connector. It would not make sense to install the connectors through the lid either because opening the case may place too much tension on the wires causing damage.

It will also be important to orient the breadboard in a manner that the accelerometer measures data in the intended direction as if it was mounted. Otherwise, it will need to be understood that the data measured on each axis during lab trials will not be measured along the same axes in the field and will need to be accounted for while analyzing the data.

### Package Location

## 6.3 Package Location

Figure 6.10 is an Abaqus visualization of the Newport Bridge with the proposed location for the sensor package to be mounted. As shown in the figure, the center of the bridge is the best location for the sensor package. This is because the greatest amplitude of displacement will occur during the first mode of vibration at the middle of the bridge. Mounting the sensor package to the bridge must be done without damaging the structure in any way. The sensor package must also be capable of being moved easily. Most importantly, the package must be secured without any of its own motion so that the sensors can recognize the movement of the bridge and not the movement of the package itself.

The most economical way of securing the sensor package to the bridge is to use powerful magnets. Neodymium Magnets are strong magnets that work well in all environments and resist demagnetization. One negative aspect of magnets is that they can be prone to corrosion

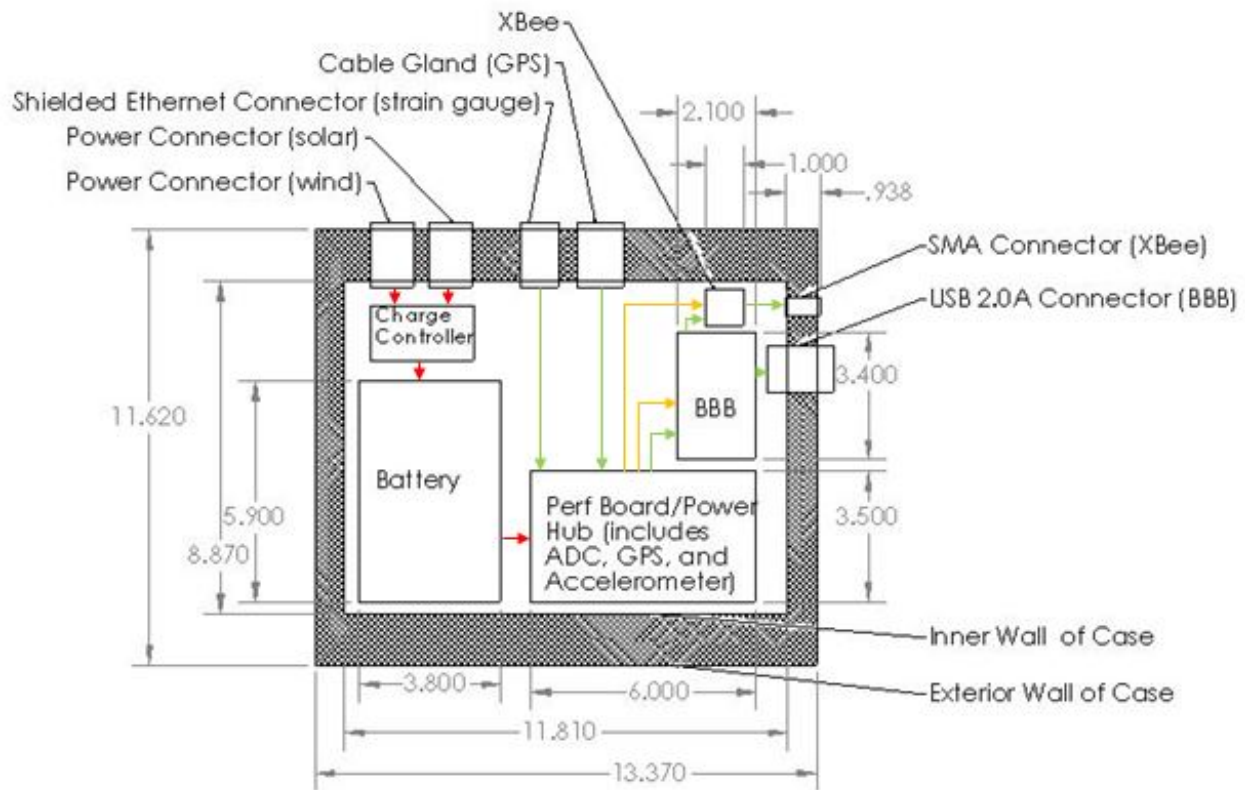


Figure 6.8: Potential Layout of a Pelican 1400 Model Case

if a protective coating is not properly applied. There is also a concern that the magnetic field can disrupt the electronics within the case. However, these issues can be prevented if the correct precautions are taken. These magnets come in many shapes and sizes, as shown in Figure 6.9, and can be purchased with pre-fabricated holes for screws to attach the magnets to the exterior of the case. The magnets in figure 6.9 are the MMR-A-XC model of magnets from KJMagnetics.com. This magnet is hardly larger than a penny, yet it can easily be screwed into the sensor package and has a holding force of 54.14 pounds. With two of these magnets screwed into the case, the package would be secured to the bridge. If data analysis is performed to prove the wind speed on the surface of the package to be too much for this pull force, stronger magnets are available. KJMagnetics.com also has similar magnets but with different pull forces ranging from 26.8 pounds to 260 pounds. These magnets can be used for securing the solar panels and wind turbine as well.

Figure 6.11 shows a practicable location for the sensor package along with the solar panels above and the wind turbine hanging just below. The sensor package should be mounted on the outside of one of the major vertical beams at midspan of the bridge. The solar panels and wind turbine must be mounted close within a reasonable distance to keep the cable length to a minimum. The best place to mount the solar panels is on top of the upper horizontal beam on the southern side of the bridge. This will allow for the most amount of sun light and the shortest amount of cable necessary. The best place to mount the wind turbine is on the bottom of the lower horizontal beam on the southern side of the bridge. This location

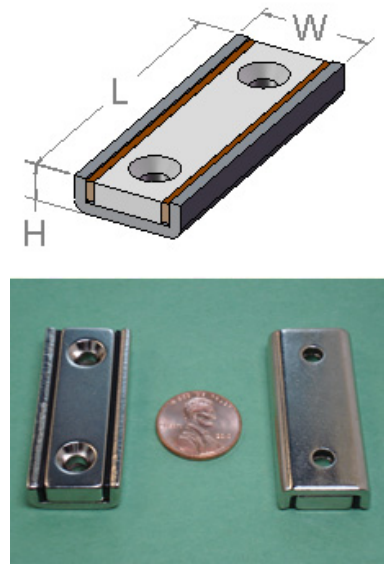


Figure 6.9: Neodymium Mounting Magnet.

has plenty of wind because it is above the middle of the Narragansett Bay. By mounting the sensor package, solar panels and wind turbine below the deck on the southern side of the bridge the package will be capable of producing its own power and accurately measuring the vibrations of the bridge.



Figure 6.10: Proposed Package Mounting Location.

## 6.4 FEM

### 6.4.1 Model Improvements

### 6.4.2 Dynamic Loading

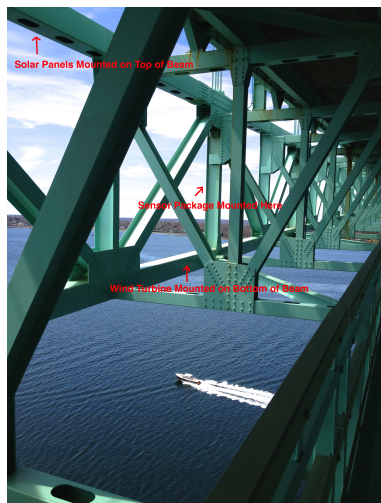


Figure 6.11: Proposed Location for Sensor Package, Wind Turbine and Solar Panels.

# **Chapter 7**

## **Conclusion**

# Bibliography

- [1] G. Gareis. Surfaced cable filler, December 18 2003. US Patent App. 10/425,502.
- [2] Bruce Hunter and Patrick Rowland. *Linear Regulator Design Guide for LDOs*. Texas Instruments, June 2008.

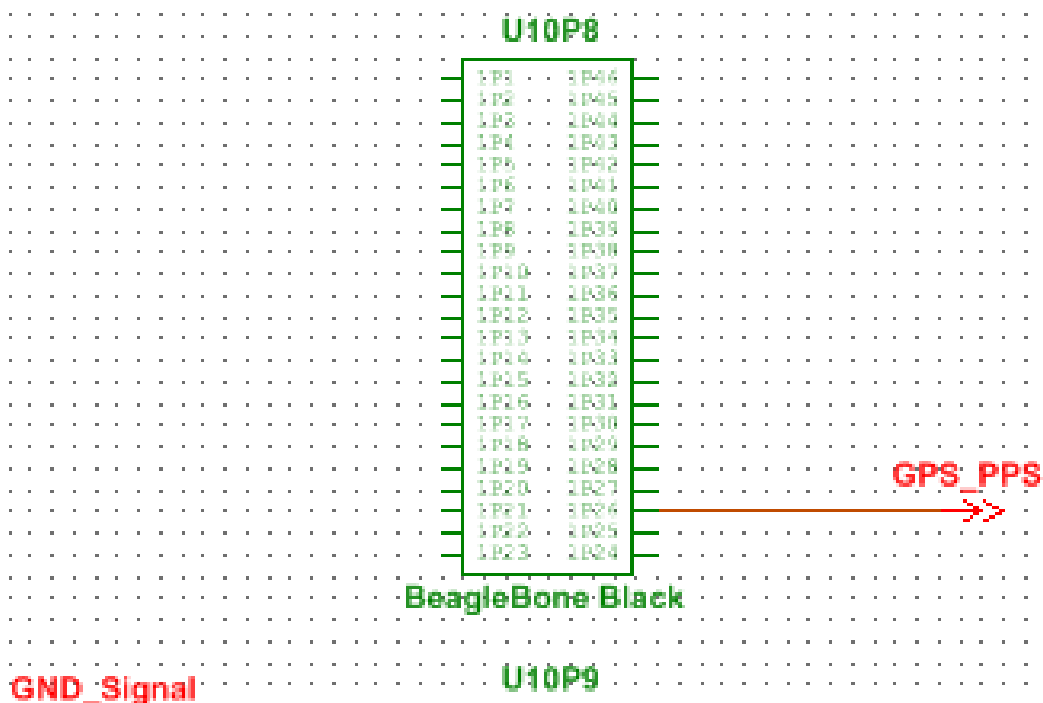


# Appendix A

## Sensor Package Schematics

### A.1 BeagleBone Black

# BeagleBone Black Block



## A.2 Trimble Copernicus II GPS Receiver

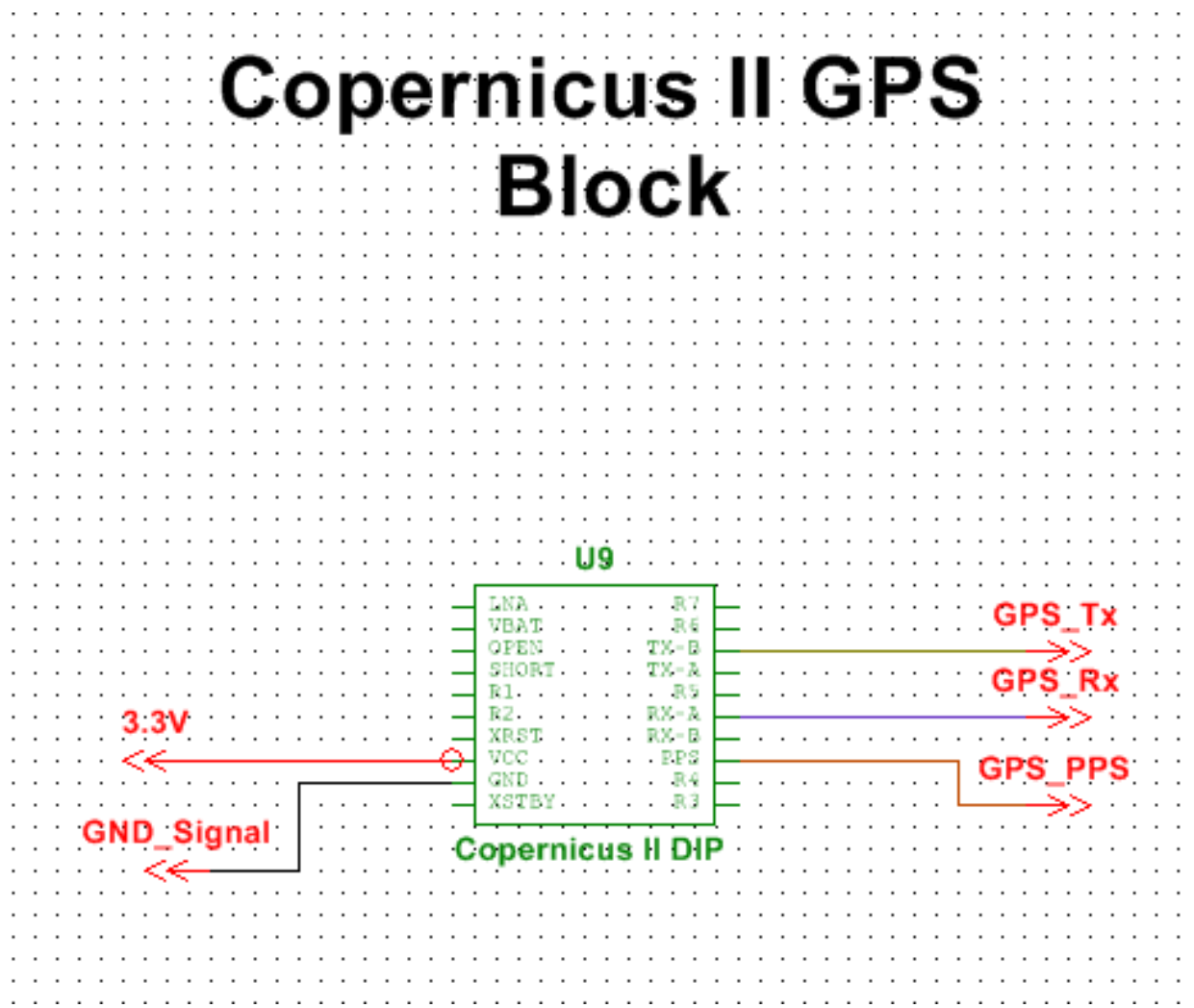


Figure A.2: Schematic of Copernicus II GPS Receiver



### A.3 ADS1113 Analog-Digital Converter

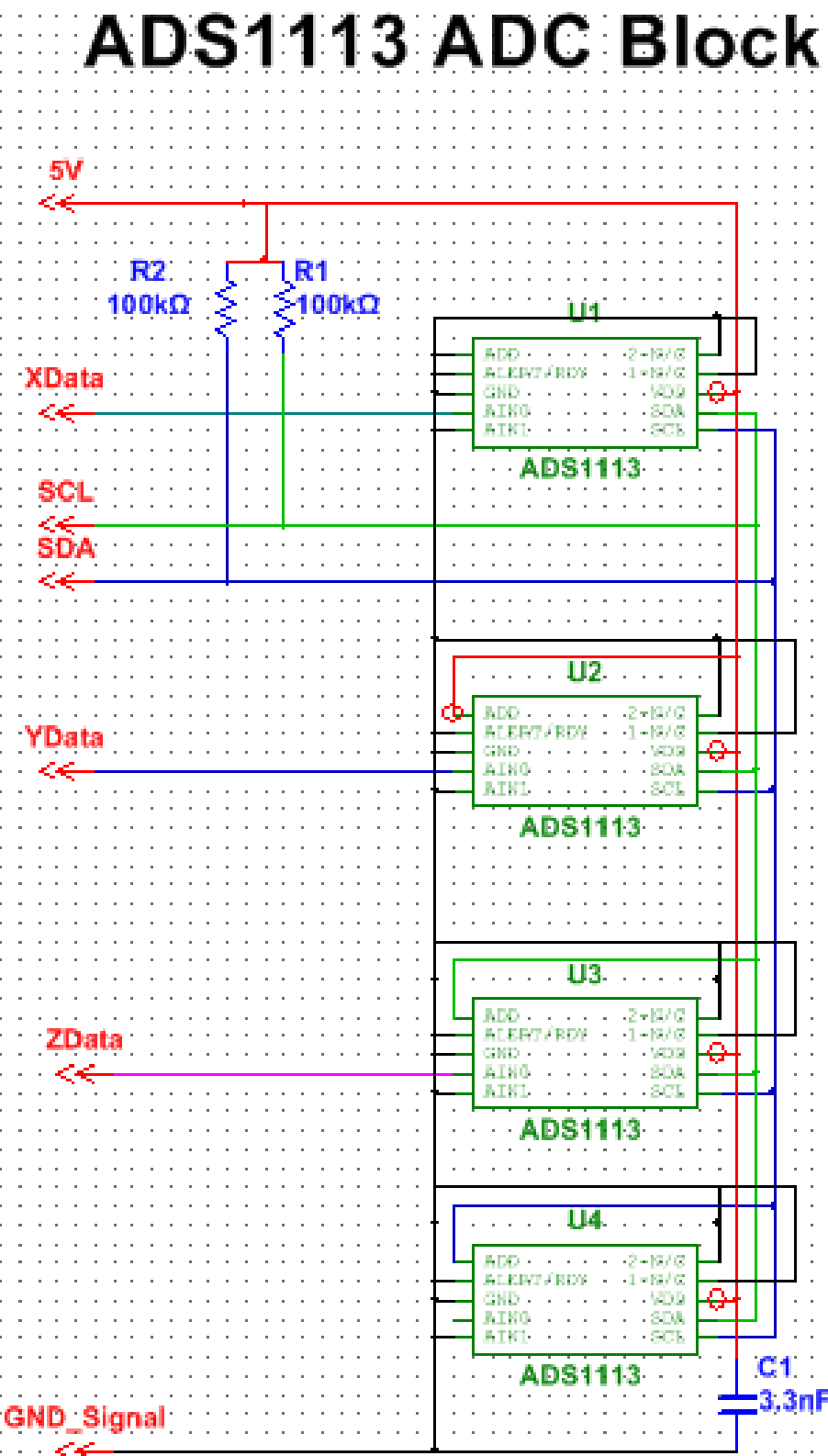


Figure A.3: Schematic of four ADS1113 ADC units in parallel

## A.4 LM317 Adjustable Voltage Regulators

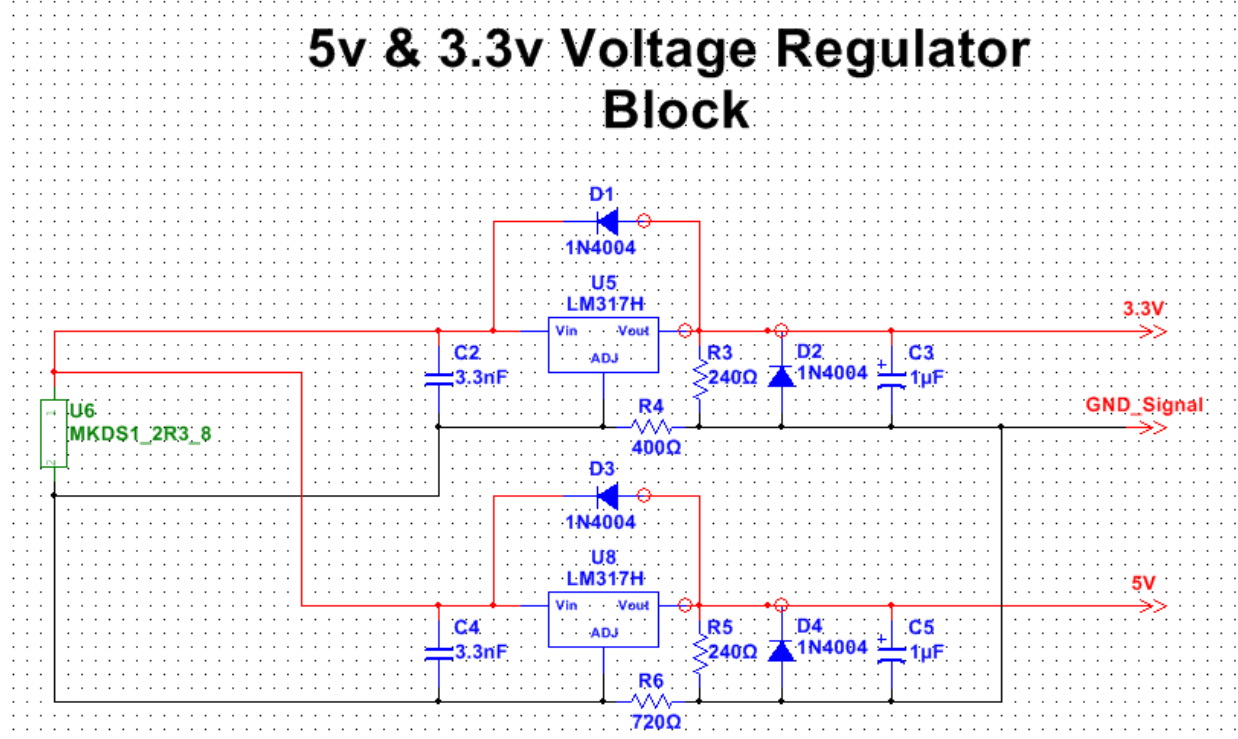


Figure A.4: Schematic of 5V and 3.3V voltage regulator circuit

## A.5 MMA7361 Accelerometer

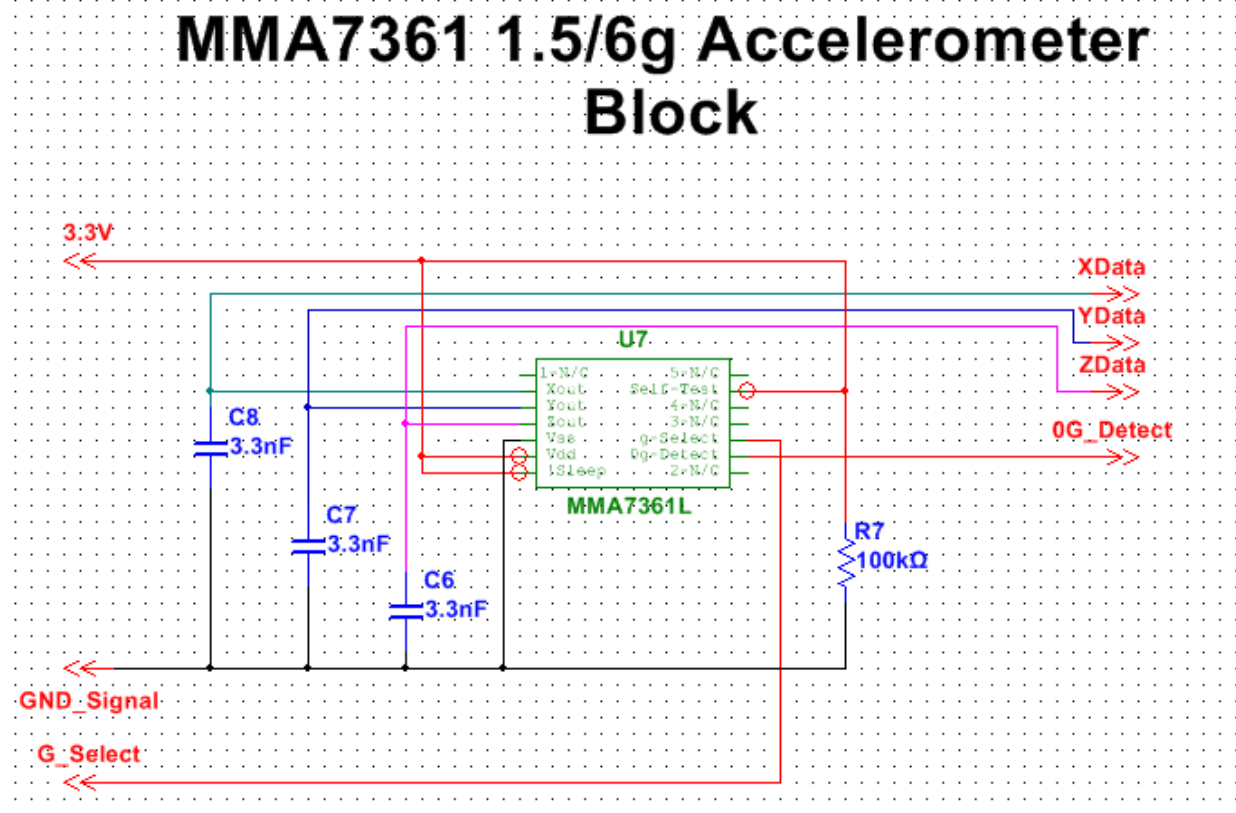


Figure A.5: Schematic of MMA7361  $\pm 1.5g$  /  $\pm 6g$  Tri-Axial Accelerometer

# **Appendix B**

## **Enclosure Options**

Company	Case Model	Enclosure Options					Cost	Thermal Conductivity Coefficient (W/m*°C)
		Length	Width	Height	Weight			
Pelican	1300	9.17	7.00	6.12	3.09	\$55.65	0.1-0.22	
	1400	11.81	8.87	5.18	3.97	\$81.58	0.1-0.22	
	1450	14.62	10.18	6	5.51	\$103.73	0.1-0.22	
	1460	18.54	9.92	10.92	8.75	\$180.59	0.1-0.22	
	PC MH 125 G	9.1	5.5	4.9	NA	NA	0.19	
Fibox	PC 2828 18 G	10.9	10.9	7.1	NA	NA	0.19	
	PC 175/150 XHG	7.1	7.1	5.9	NA	NA	0.19	
	9.4	9.4	7.4	5.5	3.3	\$38.95	0.1-0.22	
Namuk	915	13.8	9.3	6.2	4.4	\$63.95	0.1-0.22	
	UW Kinetics Ultra-case 613	13.4	8.9	5.6	4.5	\$148.99	0.2	

Table B.1: Brief summary of enclosure options considered for the sensor package